



Efficient activation of sulfite for reductive-oxidative degradation of chloramphenicol by carbon-supported cobalt ferrite catalysts

Yongjie Li^a, Mingjie Huang^{a,*}, Wen-Da Oh^b, Xiaohui Wu^a, Tao Zhou^{a,*}

^a School of Environmental Science and Engineering, Huazhong University of Science and Technology, Wuhan 430074, China

^b School of Chemical Sciences, Universiti Sains Malaysia, Penang 11800, Malaysia

ARTICLE INFO

Article history:

Received 20 September 2022

Revised 6 February 2023

Accepted 19 February 2023

Available online 22 February 2023

Keywords:

Cobalt ferrite spinel

Sulfite activation

Reductive dechlorination

Carbon supports

Sulfur oxygen radical reactions

ABSTRACT

Activation of (bi)sulfite (S(IV)) by metal oxides is strongly limited by low electrons utilization. In this study, two carbon-supported cobalt ferrites spinels (CoFe₂O₄ QDs-GO and CoFe₂O₄ MOFs-CNTs) have been successfully synthesized by one-step solvothermal method. It was found that both catalysts could efficiently activate S(IV), with rapid reductive dechlorination and then oxidative degradation of a recalcitrant antibiotic chloramphenicol (CAP). Characterizations revealed that CoFe₂O₄ spinels were tightly coated on the carbon bases (GO and CNTs), with effectiveness of the internal transfer of electrons. O₂^{•-} was identified for the reductive dechlorination of CAP, with simultaneously detection of both [•]OH and SO₄^{•-} responsible for further oxidative degradation. The sulfur oxygen radical conversion reactions and molecular oxygen activation would occur together upon the carbon-based spinels. Spatial-separated interfacial reductive-oxidation of CAP would occur with dechlorination of CAP by O₂^{•-} on the carbon bases, and oxidative degradation of intermediates by SO₄^{•-}/[•]OH upon the CoFe₂O₄ catalysts.

© 2023 Published by Elsevier B.V. on behalf of Chinese Chemical Society and Institute of Materia Medica, Chinese Academy of Medical Sciences.

As a broad-spectrum halogenated antibiotic highly active against Gram-positive/negative bacteria, chloramphenicol (CAP) has been banned by many countries for use in food-producing animals [1]. However, abuse of halogenated antibiotics in the past decades has posed a serious threat on human health and the environment, owing to their potential carcinogenicity and production of antibiotic resistant bacteria [2]. It is well known that CAP is strongly recalcitrant to the conventional wastewater treatment technologies, because of its stable molecular structure and biotoxicity to activate sludge [3]. Advanced oxidation processes (AOPs) based on the generation of highly reactive hydroxyl radical ([•]OH) and/or sulfate radical (SO₄^{•-}) have been widely acknowledged as good alternatives for effectively destructing halogenated antibiotics [4]. As compared to the non-selective [•]OH, SO₄^{•-} presents advantages including higher oxidation potential (2.5–3.1 V) in a wide pH range and longer half-life (30–40 μs) [5], performing more selectively with the organic compounds containing unsaturated bonds or aromatic π electrons [6,7].

Recently, a novel AOP based on (bi)sulfite (HSO₃⁻/SO₃²⁻, S(IV)) has received great attentions [8], since S(IV) can generate SO₃^{•-} and SO₄^{•-} by catalytic autooxidation process, equipped with the

superiority of easy access and low cost [8,9]. However, the electron transfer pathways from S(IV) to SO₄^{•-} are long with interference side reactions, generally resulting in poor electron utilization (SO₄^{•-} yield) rate of S(IV) [10,11]. Studies concerning heterogeneous catalysts of metal oxides such as α-Fe₂O₃, CuO, MnO₂ and Co₃O₄, have been reported in improving the activation of S(IV) [12,13]. Among them, spinel CoFe₂O₄ was demonstrated to be effective for initializing S(IV) autooxidation to degrade metoprolol [14]. Despite the fact that Co/Fe bimetallic organic frameworks (MOFs) [15,16] and the Co-Fe oxides quantum dots (QDs) [17] have achieved high catalytic activities of S(IV), rational utilization of the simultaneously generated reduced metal ions and the co-existing O₂ is rarely mentioned [18,19]. In the past years, synthesis of metal-carbon based hybrids such as cobalt embedded nitrogen-rich carbon nanotubes (Co@NC), has been found as a promising way to enhance the catalytic performances of metal (oxides) [20–22].

In this study, two modified cobalt ferrite (CoFe₂O₄ QDs and CoFe₂O₄ MOFs) combined on two carbon materials (carbon nanotubes (CNTs) and graphene oxide (GO)) were successfully synthesized by simple solvothermal method, respectively. Two CoFe₂O₄-carbon catalysts, i.e., CoFe₂O₄ QDs-GO and CoFe₂O₄ MOFs-CNTs could be efficient in activating S(IV) for rapid dechlorination of CAP. It indicated that carbon-based spinels would be able to achieve the sulfur oxygen radical conversion reactions and molecular oxygen

* Corresponding authors.

E-mail addresses: huangmingjie@hust.edu.cn (M. Huang), zhoutao@hust.edu.cn (T. Zhou).

activation together, probably achieving the reductive-oxidation of halogenated antibiotics.

Both CoFe_2O_4 QDs-GO and CoFe_2O_4 MOFs-CNTs were prepared by a facile hydrothermal strategy and subsequent calcination [23,24]. For synthesizing CoFe_2O_4 QDs-GO, 2.0 mmol $\text{Fe}(\text{NO}_3)_3 \cdot 9\text{H}_2\text{O}$, 1.0 mmol $\text{Co}(\text{NO}_3)_2 \cdot 6\text{H}_2\text{O}$ and 0.75 mmol sodium citrate were dissolved in 100 mL deionized water at 50 °C and stirred for 30 min to form a clear solution. Subsequently, 25 mL of 15% $\text{NH}_3 \cdot \text{H}_2\text{O}$ was added dropwise, held at 70 °C for 2 h, then 100 mg GO and 50 mL absolute ethyl alcohol were added, followed by 1 h of sonication. The resulted fuscous slurry was transferred to a 100-mL Teflon-lined stainless autoclave, sealed and maintained at 180 °C for 20 h. The cooled back products were washed and dried overnight in vacuum at 60 °C. Finally, the as-prepared product was annealed at 450 °C for 2 h in Ar atmosphere. As for making CoFe_2O_4 MOFs-CNTs, 0.83 mmol of $\text{CoCl}_2 \cdot 6\text{H}_2\text{O}$ and 1.66 mmol $\text{Fe}(\text{NO}_3)_3 \cdot 9\text{H}_2\text{O}$ were mixed in 4 mL ethyl alcohol and 4 mL deionized water to obtain solution A. Meanwhile, 0.06 g CNTs was intensively dissolved in 53 mL DMF (*N,N*-dimethylformamide) with addition of 1.1327 g DHTA (2,5-dihydroxyterephthalic acid) (solution B). The two obtained solutions were uniformly mixed and transferred to a 100 mL Teflon container at 135 °C for 24 h. The cooled product was centrifuged three times using methanol and dried at 80 °C for 24 h, followed by calcination at 800 °C for 2 h at a rate of 5 °C/min in air.

Morphologies of the two catalysts were characterized by a field emission-scanning electron microscopy (FE-SEM, EM3900M, ZEISS, Germany) and a high-resolution transmission electron microscopy (HR-TEM, Tecnai G2 F30 transmission electron microscope). X-ray diffraction (XRD) was performed on a Seifert Iso-DebyeFlex 2002 diffractometer using $\text{Cu-K}\alpha$ radiation (wavelength = 1.54 Å). The generated reactive oxygen species (ROS) were examined by an Electron paramagnetic resonance spectrometer (EPR, MEX-nano, Bruker), the modulation frequency was 100 kHz and the microwave power were 15 mW. Quantifications of the concentration of CAP and released free chloride were carried out by a HPLC [25] and an ion chromatography (Thermo Scientific - Dionex ICS-1600, Metrosep A Supp 7-250 (250×4 mm) column with 1.2 mL/min $\text{Na}_2\text{CO}_3/\text{NaHCO}_3$ (4.5 mmol/L/1.4 mmol/L) as eluent), respectively. Total organic carbon (TOC) of the solution was analyzed using a multi TOC/TN 2100 Analyzer (Analytik Jena AG Corporation).

The degradation experiments of CAP were performed in a 250 mL beaker at 25 °C. In a typical experiment run, the reaction was started as adding 0.1 g/L of CoFe_2O_4 QDs-GO or CoFe_2O_4 MOFs-CNTs into 250 mL reaction solution contain 10 mg/L CPA and 0.2 mmol/L Na_2SO_3 , the initial reaction pH was set as 9.0 [22]. The scavenging experiments were conducted with 500 mmol/L methanol (MeOH), *tert*-butyl alcohol (TBA) or 1500 U/mL superoxide dismutase (SOD), respectively.

Fig. 1a shows that the CoFe_2O_4 QDs nanoparticles (5–20 nm, Fig. 1b) has been successfully coated on the surface of GO, with partly irregular agglomerations. HR-TEM image of the CoFe_2O_4 QDs-GO revealed the good combination of the CoFe_2O_4 QDs and GO base, with nanoparticles fringe spacings of 0.258 nm, which correspond to the interplanar CoFe_2O_4 QDs (311) direction. Fig. 1c exhibits a spindle like morphology wrapped around CNTs for the CoFe_2O_4 MOFs-CNTs. The related size of CoFe_2O_4 MOFs was in the range of 2–3 μm (Fig. 1d), and CNTs was successfully coated upon the MOFs.

UV-vis DRS measurements of the two comparative materials groups (Figs. 1e and f, Figs. S1a-f in Supporting information) revealed that the calculated E_g values were 1.97, 3.03, 4.09 eV, and 2.65, 2.63, 2.89 eV, respectively, corresponding to CoFe_2O_4 QDs, CoFe_2O_4 QDs-GO, GO, and CoFe_2O_4 MOFs, CoFe_2O_4 MOFs-CNTs, CNTs. This suggested that the electron-transfer efficiency in the carbon-based CoFe_2O_4 catalysts would be effectively improved, since the solid containing Fe^{3+} and Co^{2+} ions could introduce a new

level approaching to the conduction [26]. Figs. 1g and h showed XRD patterns of the above materials, where the characteristic peaks (220), (311), (400), (333), and (440) could be attributed to the cobalt ferrite structure agreeing with the JCPDS (#22-1086) data [27]. GO characteristic peaks (002) and structure of Fe-MIL-88A can be also found in the spectra of CoFe_2O_4 QDs-GO and CoFe_2O_4 MOFs-CNTs, respectively.

Furthermore, the FTIR spectra of the two carbon-based catalysts (Figs. 1i and j) indicates appearance of two peaks at 1390 and 1560 cm^{-1} , corresponding to symmetric and asymmetric stretching vibrations of COO^- groups, respectively. The presence of typical Fe-O and Co-O vibrations, which centered at around 609 and 872 cm^{-1} [28], could assert the attendance of Fe and Co metals in the CoFe_2O_4 spindles. In addition, the existence of surface hydroxyl (OH) groups on CoFe_2O_4 QDs-GO and CoFe_2O_4 MOFs-CNTs could be confirmed by the presence of a broad band at around 3420 cm^{-1} [29].

Fig. 2a illustrates the time-dependent degradation of CAP in four comparative systems, i.e., the CoFe_2O_4 QDs-GO, GO/ Na_2SO_3 , CoFe_2O_4 QDs/ Na_2SO_3 , CoFe_2O_4 QDs-GO/ Na_2SO_3 systems. It was found that the removal of CAP was negligible in the CoFe_2O_4 QDs-GO alone system, indicating that CoFe_2O_4 QDs-GO was difficult to absorb CAP or activate O_2 . Both GO/ Na_2SO_3 and CoFe_2O_4 QDs/ Na_2SO_3 systems could rapidly degrade a few of CAP in the initial reaction time, but tended to slow degradation patterns afterwards. This suggested that the fresh surface sites upon GO or CoFe_2O_4 QDs could activate S(IV), while they were fast consumed or covered. Moreover, the CoFe_2O_4 QDs-GO/ Na_2SO_3 system could achieve a significant synergy in the CAP degradation with a pseudo first-order kinetic constant (k_{obs}) of $3.67 \times 10^{-2} \text{ min}^{-1}$, which was 6.1, 6.7 and 6.4 times larger than of the GO/ Na_2SO_3 , CoFe_2O_4 QDs/ Na_2SO_3 and CoFe_2O_4 QDs+GO (mechanical mixing) S(IV) activation systems (Fig. S2a in Supporting information). This result demonstrated that chemical coupling of CoFe_2O_4 QDs and GO could greatly enhance the catalytic activation of S(IV) in the system, possibly accompanying with obviously improved utilization of the generated electrons [30].

Fig. 2b shows the simultaneous released chloride and consumed sulfite in the above four comparative systems after 1 h of the reaction time. It was very interesting to note that the CoFe_2O_4 QDs-GO/ Na_2SO_3 system could lead to an amazing amount of dissolved chloride as 0.030 mmol/L that was related closely to the degradation of initial 10 mg/L CAP (Fig. 2a). However, marginal amounts (< 1 μmol) of chloride were detected in the other three systems, indicating that the traditional activation of S(IV) by either spinels (CoFe_2O_4 QDs) or carbon base materials (GO) would be not able to induce direct reductive dechlorination of the recalcitrant CAP. Moreover, it was also observed that the consumptions of sulfite well correlated with their degradation amounts of CAP in the above four systems (Figs. 2a and b), at related stable molar ratio $\Delta[\text{S(IV)}]/\Delta[\text{CAP}]$ of about 6.5. This indicated that S(IV) was the predominant electron contributor for CAP decomposition, and the modification engineering between CoFe_2O_4 QDs and GO would alter the electron utilization pathway of S(IV) activation to induce the efficient direct dichlorination [31].

Fig. 2c exhibits the time-dependent CAP degradation in the four comparative systems of CoFe_2O_4 MOFs and CNTs. Similar patterns were observed as compared to the above GO groups. The material CoFe_2O_4 MOFs-CNTs could absorb marginal amount of CAP (< 5.0%), and either CNTs or CoFe_2O_4 MOFs alone could only degrade no more than 30.0% of the initial CAP. The mechanical mixing of them (CoFe_2O_4 MOFs + CNTs) could not bring any synergy (Fig. S2a). Like above, the CoFe_2O_4 MOFs-CNTs/ Na_2SO_3 system achieved great synergy in the CAP degradation, with the k_{obs} of $3.45 \times 10^{-2} \text{ min}^{-1}$, that was 7.7, 5.1 and 8.2 times larger than of the CNTs, CoFe_2O_4 MOFs, and CoFe_2O_4 MOFs+CNTs S(IV) activation systems. It

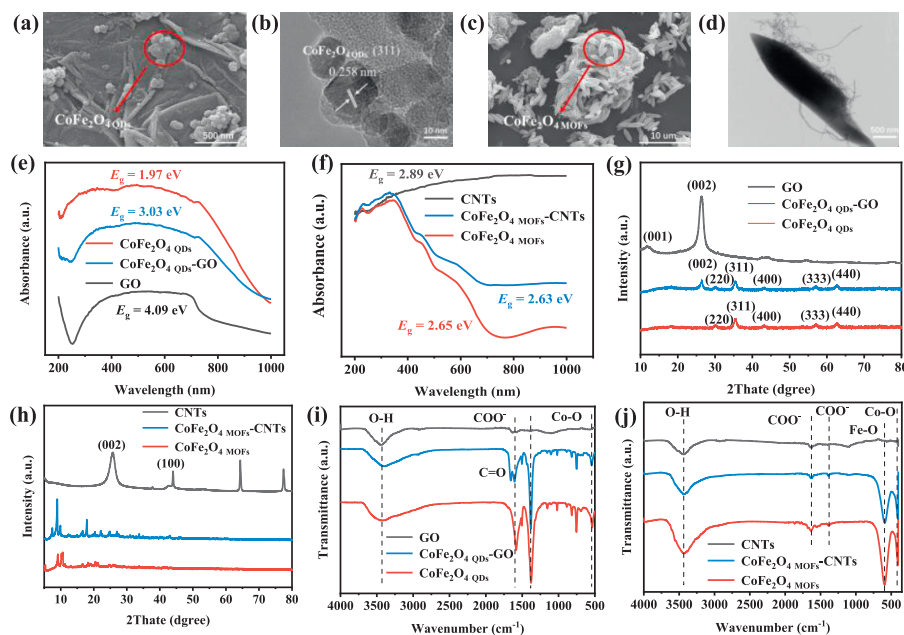


Fig. 1. SEM and HR-TEM images of (a, b) CoFe₂O₄ QDs-GO and (c, d) CoFe₂O₄ MOFs-CNTs, respectively. UV-vis DRS spectra (e, f), XRD (g, h) and FTIR patterns (i, j) of the two comparative materials groups (CoFe₂O₄ QDs-GO and CoFe₂O₄ MOFs-CNTs).

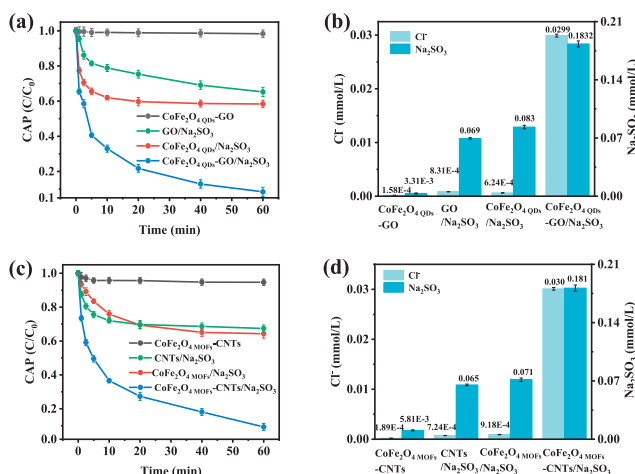


Fig. 2. Comparative CAP degradation and the related chloride releases with Na₂SO₃ consumptions in the comparative systems: (a, b) CoFe₂O₄ QDs-GO, GO/Na₂SO₃, CoFe₂O₄ QDs/Na₂SO₃, CoFe₂O₄ QDs-GO/Na₂SO₃, and (c, d) CoFe₂O₄ MOFs-CNTs, CNTs/Na₂SO₃, CoFe₂O₄ MOFs/Na₂SO₃, CoFe₂O₄ MOFs-CNTs/Na₂SO₃ systems. Initial conditions were: 0.1 g/L catalyst, 0.2 mmol/L Na₂SO₃, 10 mg/L CAP, pH 9.0 and 25 °C.

also demonstrated that the chemical connection between CNT and MOFs (Co-Fe) would improve the catalytic activity of S(IV) activation. Furthermore, the related results of chloride release and S(IV) consumption evidenced that the rapid reductive dechlorination of CAP occurred only in the CoFe₂O₄ MOFs-CNTs/Na₂SO₃ system, even the $\Delta[S(IV)]/\Delta[CAP]$ were all at 6.7–7.2 for the four comparative systems (Figs. 2c and d). It suggested that the adoption of different types of carbon bases would be capable of inducing shift of the electrons transfer pathway from sole S(IV) activation to plus O₂ activation [32].

As shown in Figs. S3a and b (Supporting information), negligible total organic carbon (TOC) removal occurred in the CoFe₂O₄ QDs-GO, GO/Na₂SO₃, and CoFe₂O₄ QDs/Na₂SO₃ system, indicating that the catalyst adsorption and direct oxidation could hardly con-

tribute to the mineralization of CAP. In contrast, ~70% of TOC was removed in the CoFe₂O₄ QDs-GO/Na₂SO₃ and CoFe₂O₄ MOFs-CNTs/Na₂SO₃ systems, which validated that the reductive and oxidative strategy proposed in this study could lead to greatly enhanced mineralization of CAP. The effect of pH on CAP degradation was also conducted. As shown in Fig. S4 (Supporting information), with the pH increased from 3 to 9, the CAP degradation efficiency first increased and then decrease in both the CoFe₂O₄ QDs-GO and CoFe₂O₄ MOFs-CNTs catalytic systems. The optimal pH value for sulfite activation is 9 (Figs. S4a and b).

Other two carbon-based catalysts, i.e., CoFe₂O₄ QDs-CNTs and CoFe₂O₄ MOFs-GO were also synthesized by similar solvothermal methods (Supporting information). Although the CAP degradation in the two cases was not good, similarly effective releases of chloride were found (Figs. S2b and c in Supporting information). This confirmed that the carbon bases could induce the generated electrons from S(IV) activation to reduce their surface absorbed oxygen [14], but the CoFe₂O₄ sites for the S(IV) activation may be restricted due to inappropriate synthesis procedures [33].

Generation of ROS involved the CAP degradation in the related systems were examined by EPR and radical quenching experiments. Notably, strong signals of O₂^{•-}, [•]OH and SO₄^{•-} were detected in the CoFe₂O₄ QDs-GO/Na₂SO₃ and CoFe₂O₄ MOFs-CNTs/Na₂SO₃ systems, whereas only slight signals of [•]OH and SO₄^{•-} were observed in other four S(IV) activation systems, as depicted in Figs. 3a-d. It revealed that single-electron reductive activation of O₂ on the base GO/CNTs would occur in the two systems by obtaining electrons transferred from the S(IV) activation on CoFe₂O₄ QDs/MOFs. The generated O₂^{•-} could lead to reductive dechlorination of CAP and efficiently release free chloride (Figs. 2b and d) [34]. Meanwhile, the two CoFe₂O₄-carbon/Na₂SO₃ systems also produced more amounts of [•]OH and SO₄^{•-} during the S(IV) activation reactions, which could cause rapid oxidative mineralization of the dechlorinated CAP intermediates. To validate the role of SO₃^{•-}, EPR spectra with or without CAP in CoFe₂O₄ MOFs-CNTs/Na₂SO₃ and CoFe₂O₄ QDs-GO/Na₂SO₃ systems were conducted. As shown in Figs. S5a and b (Supporting information), both the CoFe₂O₄ QDs-GO and CoFe₂O₄ MOFs-CNTs could activate sulfite to produce SO₃^{•-} free radical, but the addition of CAP

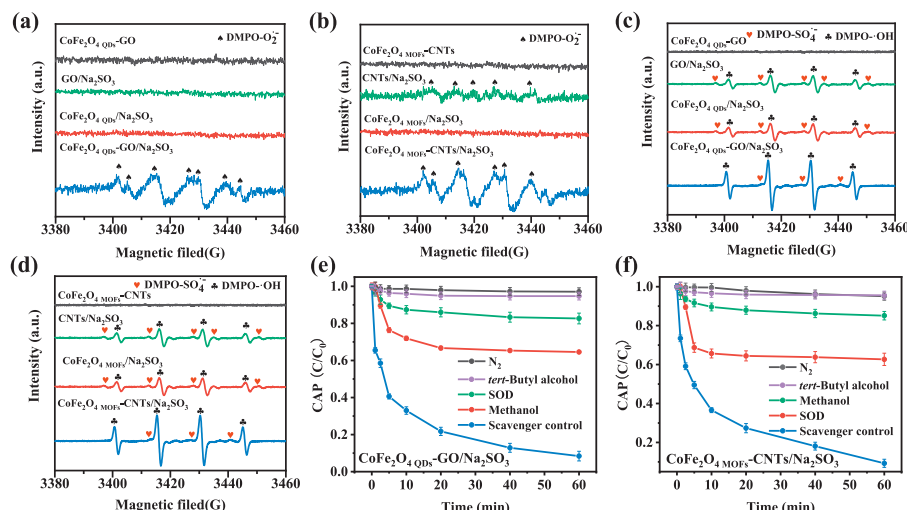


Fig. 3. DMPO spin-trapping EPR spectra with (a, b) or without methanol solvent (c, d) in the eight systems (the comparative groups of CoFe_2O_4 QDs-GO and CoFe_2O_4 MOFs-CNTs with Na_2SO_3 or not). (e, f) Effect of N_2 sparging, methanol or SOD scavengers in on CAP degradation in the CoFe_2O_4 QDs-GO and CoFe_2O_4 MOFs-CNTs systems with Na_2SO_3 . Initial conditions were: 0.1 g/L catalyst, 0.2 mmol/L Na_2SO_3 , 10 mg/L CAP, pH 9.0 and 25 °C.

posed negligible effect on the signal intensity of $\text{SO}_3^{\cdot-}$, indicating that $\text{SO}_3^{\cdot-}$ was not involved in the dechlorination and degradation of CAP. $\text{SO}_5^{\cdot-}$ were not detected by EPR. It is generally considered that $\text{SO}_5^{\cdot-}$ has no dehalogenation ability and its oxidation ability is rather weaker than that of $\cdot\text{OH}$ or $\text{SO}_4^{\cdot-}$ [35].

Figs. 3e and f show that introduction of either MeOH, TBA or N_2 sparging strongly inhibited the degradation of CAP in the CoFe_2O_4 QDs-GO and CoFe_2O_4 MOFs-CNTs S(IV) activation systems, respectively. It suggested that both $\cdot\text{OH}$ and $\text{SO}_4^{\cdot-}$ were the main ROS for CAP degradation in S(IV) systems, while O_2 would crucially participate in the $\text{SO}_4^{\cdot-}$ generation reactions [36]. Interestingly, SOD, a common consumer for $\text{O}_2^{\cdot-}$ [37], could only partly inhibit the CAP removal, presenting degradation patterns similar to the CoFe_2O_4 QDs/MOFs/ Na_2SO_3 systems (Figs. 2a and c) and also negligible releases of chloride (Figs. S6a and b in Supporting information). However, trace of Cl^- were detected in both MeOH systems. The above result evidenced that the generated $\text{O}_2^{\cdot-}$ would be predominant for the reductive dechlorination of CAP, followed by subsequent ($\cdot\text{OH}$ and $\text{SO}_4^{\cdot-}$) oxidative degradation [38–40].

It was found that the dissolution of Co and Fe ions were very trace and less than 10% of CAP was degraded with the homogeneous metal ions (Figs. S7a-c in Supporting information), which suggested the main heterogeneous catalytic reactions. Besides, sites-binding experiments by EDTA (Fe-Co sites) and phenanthroline (Fe sites) were conducted respectively used for judging sulfite binding-site. As shown in Fig. S7d (Supporting information), the addition of EDTA and phenanthroline exhibited more strong suppression in CAP degradation as compared to no addition catalysts, suggesting that S(IV) would prefer to bond and activated at iron sites of the catalysts.

The X-ray photoelectron spectroscopy (XPS) characterization was conducted to monitor the valence state of Co and Fe on the catalyst surface. As shown Figs. S8a-d and Table S1 (Supporting information), the valence state of Co and Fe remained unchanged after the catalytic reaction. The result evidenced that Co and Fe act as intermediaries in the process of electron transfer. To explore the stability of the catalysts, four consecutive cycles for chloramphenicol degradation using CoFe_2O_4 QDs-GO and CoFe_2O_4 MOFs-CNTs were conducted, the results were displayed in Figs. S9a and b (Supporting information). It can be found that the catalytic activity of the CoFe_2O_4 QDs-GO catalyst decreases lightly, which might be

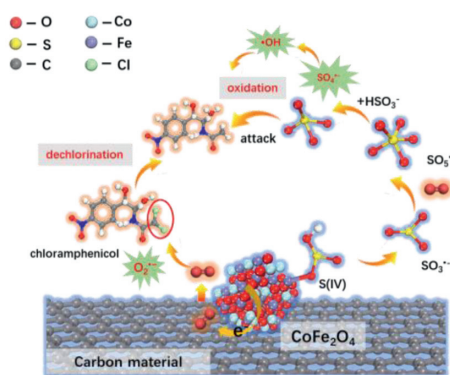


Fig. 4. A proposed mechanistic scheme of the spatial-separated reductive-oxidation of CAP in carbon-based CoFe_2O_4 catalysts/S(IV) systems.

attributed to the detachment of the CoFe_2O_4 QDs component. Besides, the CoFe_2O_4 QDs-GO catalyst shows a good stability for sulfite activation and chloramphenicol degradation. These results indicate that the origin of the active component could lead to different catalytic stability [41].

A schematic for the reaction mechanism in the two carbons based CoFe_2O_4 S(IV) activation systems could be therefore proposed as presented in Fig. 4. The sulfur oxygen radical conversion reactions and molecular oxygen activation would occur together upon the carbon-based spinels. S(IV) was first activated at surface of the bonded CoFe_2O_4 the effective separation of generated electrons, followed by fast electrons transferring to the carbon bases and *in-situ* generation of $\text{SO}_3^{\cdot-}$ and then the sulfur oxygen radical reactions ($\text{SO}_3^{2-} \rightarrow \text{SO}_3^{\cdot-} \rightarrow \text{SO}_5^{\cdot-} \rightarrow \text{SO}_4^{\cdot-}$). Meanwhile, the absorbed O_2 would obtain the electrons to generate $\text{O}_2^{\cdot-}$. Afterwards, spatial-separated interfacial reductive-oxidation of CAP would occur with dechlorination of CAP by $\text{O}_2^{\cdot-}$ on the carbon bases, and oxidative degradation of the dechlorinated intermediates by $\text{SO}_4^{\cdot-}/\cdot\text{OH}$ upon the CoFe_2O_4 catalysts.

This study has provided novel and easily prepared carbon-spinels composite catalysts for S(IV) activation. It is of great importance to develop an innovative catalytic oxidation technology with the dual-function of reductive dehalogenation and oxidative degradation of recalcitrant halogenated antibiotics.

Declaration of competing interest

The authors declare that they have no known competing financial interests or personal relationships that could have appeared to influence the work reported in this paper.

Acknowledgments

This study is financially-supported by the National Natural Science Foundation of China (Nos. 21677055, 22006045 and 21407052), the National Key Technical Research and Development Program of China (No. 2019YFC1805204), Leading Plan for Scientific and Technological Innovation of High-tech Industries of Hunan Province (No. 2021GK4060) and the Fundamental Research Funds for the Central Universities, HUST (No. 2017KFXKJC004). Huazhong University of Science & Technology Analytic and Testing centre is thanked for the advanced analytic operations.

Supplementary materials

Supplementary material associated with this article can be found, in the online version, at doi:10.1016/j.ccllet.2023.108247.

References

- [1] X. Wang, Y. Lin, Y. Zheng, F. Meng, *Environ. Pollut.* 293 (2022) 118541.
- [2] D. Kong, B. Liang, H. Yun, et al., *Water Res.* 72 (2015) 281–292.
- [3] J. Yu, X. Hou, X. Hu, et al., *Appl. Catal. B: Environ.* 256 (2019) 117876.
- [4] M. Sun, C. Chu, F. Geng, et al., *Environ. Sci. Technol. Lett.* 5 (2018) 186–191.
- [5] U. Ushani, X. Lu, J. Wang, et al., *Chem. Eng. J.* 402 (2020) 126232.
- [6] Y. Li, W. Xiang, T. Zhou, et al., *Chin. Chem. Lett.* 31 (2020) 2757–2761.
- [7] P. Westerhoff, G. Aiken, G. Amy, et al., *Water Res.* 33 (1999) 2265–2276.
- [8] T. Liu, Z. Xie, P. Zhou, Z. et al., *Chem. Eng. J.* 431 (2022) 133464.
- [9] Y. Yuan, Oxidative of organic compounds by Oxy-sulfur radicals in the presence of transition metal ions and sulfite, Université Clermont Auvergne [2017–2020]; Université de Wuhan (Chine), 2018.
- [10] S. Wu, L. Shen, Y. Lin, et al., *Chem. Eng. J.* 414 (2021) 128872.
- [11] T. Liu, Y. Liu, P. Zhou, et al., *J. Hazard. Mater.* 440 (2022) 129809.
- [12] W.-J. Liu, E. Kwon, N.N. Huy, et al., *J. Taiwan Inst. Chem. Eng.* 133 (2022) 104253.
- [13] Q. Jing, H. Li, *Curr. Organocatal.* 7 (2020) 179–198.
- [14] Z. Liu, S. Yang, Y. Yuan, et al., *J. Hazard. Mater.* 324 (2017) 583–592.
- [15] S. Yang, X. Qiu, P. Jin, et al., *Chem. Eng. J.* 353 (2018) 329–339.
- [16] Y. Su, M. Lu, R. Su, et al., *Chin. Chem. Lett.* 33 (2022) 2573–2578.
- [17] X. Ma, P. Zhang, Y. Zhao, et al., *Chem. Eng. J.* 327 (2017) 1000–1010.
- [18] D. Zhou, L. Chen, J. Li, et al., *Chem. Eng. J.* 346 (2018) 726–738.
- [19] S. Zou, Q. Chen, Y. Liu, et al., *Chin. Chem. Lett.* 32 (2021) 2066–2072.
- [20] D. Wu, P. Ye, M. Wang, et al., *J. Hazard. Mater.* 352 (2018) 148–156.
- [21] P. Neta, R.E. Huie, *Environ. Health Perspect.* 64 (1985) 209–217.
- [22] X. Wang, X. Pu, Y. Yuan, et al., *Chin. Chem. Lett.* 31 (2020) 2634–2640.
- [23] L. Yao, H. Deng, Q.-A. Huang, et al., *J. Alloys Compd.* 693 (2017) 929–935.
- [24] H.Y. Hafeez, S.K. Lakhera, N. Narayanan, et al., *ACS Omega* 4 (2019) 880–891.
- [25] J. Han, Y. Wang, C. Yu, et al., *Anal. Chim. Acta.* 685 (2011) 138–145.
- [26] H. Ma, C. Liu, *Front. Energy.* 15 (2021) 621–630.
- [27] N.B. Velhal, N.D. Patil, A.R. Shelke, et al., *AIP Adv.* 5 (2015) 097166.
- [28] S. Yadav, S. Sharma, S. Dutta, et al., *Inorg. Chem.* 59 (2020) 8334–8344.
- [29] T. Muthukumar, J. Philip, *Colloids Surf. A* 610 (2021) 125755.
- [30] Z. Wu, Y. Wang, Z. Xiong, et al., *Appl. Catal. B: Environ.* 277 (2020) 119136.
- [31] M. Yang, Z. Hou, X. Zhang, et al., *Environ. Sci. Technol.* 56 (2022) 11635–11645.
- [32] Y. Shang, X. Liu, Y. Li, et al., *Chem. Eng. J.* 446 (2022) 137120.
- [33] Y. Shang, X. Duan, S. Wang, et al., *Chin. Chem. Lett.* 33 (2022) 663–673.
- [34] M. Huang, Y. Han, W. Xiang, et al., *Environ. Sci. Technol.* 55 (2021) 15361–15370.
- [35] G. Cai, L. Li, D. Li, et al., *Water Res.* 222 (2022) 118839.
- [36] L. Wang, H. Xu, N. Jiang, et al., *Environ. Sci. Technol.* 54 (2020) 4686–4694.
- [37] J.G. Scandalios, *Plant Physiol.* 101 (1993) 7.
- [38] C. Wang, Y. Liu, T. Zhou, et al., *Chin. Chem. Lett.* 30 (2019) 2231–2235.
- [39] W. Xiang, M. Huang, X. Wu, et al., *Chin. Chem. Lett.* 33 (2022) 1275–1278.
- [40] M. Huang, W. Xiang, C. Wang, et al., *Chin. Chem. Lett.* 31 (2020) 2769–2773.
- [41] W. Xiang, M. Huang, Y. Wang, et al., *Chin. Chem. Lett.* 31 (2020) 2831–2834.